West-East High Speed Flow Field Conference
19-22, November 2007
Moscow, Russia

LES and hybrid RANS/LES simulation of complex flows on unstructured grids

Maria-Vittoria Salvetti[1] **Simone Camarri**[1] **Bruno Koobus**[2] **Alain Dervieux**[3]

[1] *Dipartimento di Ingegneria Aerospaziale, Università di Pisa, Via G. Caruso, 56122 Pisa, Italy. mv.salvetti@ing.unipi.it, s.camarri@ing.unipi.it*
[2] *Département de Mathématiques, Université de Montpellier II, Place E. Bataillon, 34095 Montpellier, France. koobus@math.univ-montp2.fr*
[3] *INRIA, 2004 Route des Lucioles, 06902 Sophia-Antipolis, France. Alain.Dervieux@sophia.inria.fr*

Key words: hybrid RANS/LES approach, complex flows, variational multiscale LES.

Abstract. The research activity carried out by our group towards the accurate numerical prediction of complex flows is summarized. The large-eddy simulation (LES) and variational multiscale (VMS) LES approaches are adopted to simulate massively separated, three-dimensional, unsteady flows. The numerical discretization is based on a mixed finite-element/finite-volume formulation on unstructured grid. The application of the LES and VMS-LES approaches to the flow around a square cylinder at a Reynolds number equal to $Re = 22000$ is presented and analyzed. Furthermore, in order to simulate high Reynolds number flows, a new strategy for blending RANS and LES approaches in a hybrid model is described. The flow variables are decomposed in a RANS part (i.e. the averaged flow field), a correction part that takes into account the turbulent large-scale fluctuations, and a third part made of the unresolved or SGS fluctuations. The basic idea is to solve the RANS equations in the whole computational domain and to correct the obtained averaged flow field by adding, where the grid is adequately refined, the remaining resolved fluctuations. To obtain a model which progressively switches from the RANS to the LES mode, a smooth blending function is introduced to damp the correction term. Different definitions of the blending function are proposed and investigated. This approach is applied to the simulation of the flow around a square cylinder and of the flow around a circular cylinder at $Re = 140000$. Results are compared to those of other hybrid simulations in the literature and to experimental data. The sensitivity to different parameters, such as the blending function definition, the grid refinement and the closure model for the LES part, is analyzed.

1 Introduction

The most widely used approach for the simulation of *complex* turbulent flows is the one based on the Reynolds-Averaged Navier-Stokes equations (RANS). For complex flows, we mean flows characterized by complex geometry and high Reynolds

numbers, as most of the flows of industrial or engineering interest. However, RANS models usually have difficulties in providing accurate predictions for flows with massive separations, as for instance the flow around bluff bodies. An alternative approach is the Large-Eddy simulation (LES), which, for massively separated flows, is generally more accurate, but computationally more expensive, than RANS. Up to now, most of the simulations reported in the literature are limited to moderate Reynolds numbers and simple geometries and some open issues remain before LES can be considered a completely reliable tool for complex flow simulations.

The success of a large-eddy simulation depends on the combination and interaction of different factors, viz. the numerical discretization, which also provides filtering when no explicit one is applied, the grid refinement and quality and the physical closure model.

In the perspective of the application of LES in an industrial context, the use of *unstructured grids* becomes particularly attractive, because of their friendliness when applied to complex realistic geometries, although they are more demanding from the point of view of computational resources.

The *numerical accuracy* question becomes crucial with unstructured grids. Indeed, high-order approximations, such as Discontinuous Galerkin methods are quite expensive for unstructured grids. Although there are a few examples of numerical schemes especially developed for LES on unstructured grids (see e.g. Mahesh et al.[21]), our choice was to start from an existing numerical technology for industrial application and, in particular, from a *second-order co-located scheme*. The most critical point with co-located schemes is, in our opinion, the need of *numerical dissipation*. To better understand why, it is useful to examine how LES works.

The classical LES approach relies on the addition to the usual Navier-Stokes equations of a sub-grid scale (SGS) term and assumes that this same term is rather optimal for both turbulence modeling and numerical scheme stabilization. Similarly to Direct Numerical Simulation (DNS), it has been stated by many authors that the approximation should be of the highest possible accuracy order and preferably without any numerical dissipation. In that case, the damping of any high frequency component is performed exclusively by the SGS terms. It is not useless to recall that in general, these terms are second-order derivatives of the flow variables (e.g. in eddy-viscosity models), thus they introduce a rather violent damping, applied to some particular flow variables, which is however not adequate to stabilize the numerical scheme. Conversely, in a different approach, the role of SGS terms is completely fulfilled by a purely numerical stabilization term inside the approximation. A typical example is the MILES method[12] in which both subgrid modeling and numerical stabilization rely on monotonic dissipation by again a second order derivative (e.g. FCT (Flux-Corrected Transport) or TVD (Total-Variation Diminishing) schemes). However this family of model-free monotone methods seems to need a much larger number of nodes in the mesh for a given prediction quality, which is in conflict to our computational cost criterion.

Conversely, if monotone schemes are combined with a classical LES model, they can interact unfavorably with it, and significantly deteriorate the results (see, for instance, Garnier et al.[15]). Thus, it appears that in a reasonable option, the effects of numerical dissipation and of the SGS model should be separated as much as possible. Our proposition was to dedicate the subgrid modeling to a physics-based model and to use for numerics a second-order accurate MUSCL upwind scheme involving

no TVD limiters. This co-located scheme was equipped with a tunable dissipation made of *fourth-order*[7] or *sixth-order*[6] spatial derivatives of all flow variables through a flux splitting. Fourier analysis clearly shows that such a dissipation has a dissipative effect which is much more localized on high frequencies than the one of stabilizations based on second-order derivatives. In this way we can reduce the interaction between, on one hand, numerical dissipation which damps in priority the highest frequencies, in particular those for which the phase error is too large and can produce oscillations, and on the other hand SGS modeling which should reproduce the effects of unresolved frequencies on the resolved ones. Moreover, a key coefficient (γ_s) permits to tune numerical dissipation to the smallest amount required to stabilize the simulation.

As for SGS modeling, our first choice was to use *classical* models, viz. the Smagorinsky one[39] and its dynamic version.[16] As well known, we found that the dynamic model generally gives more accurate results than the Smagorinsky one (see, e.g., Camarri et al.[6,7]). However, due to the explicit filtering required in the dynamic procedure which is highly computationally demanding on unstructured grids, the increase in computational cost for the dynamic model was found to be rather dramatic, much larger than for structured grids or spectral schemes. On the other hand, a good compromise between accuracy and computational requirements was obtained through the Variational MultiScale approach (VMS), which was found to give the same accuracy as the dynamic model at costs comparable to those of the Smagorinsky model.[22] As will be described in the following, the main idea of VMS-LES is to decompose, through Galerkin projection, the resolved scales into the largest and smallest ones and to add the SGS model only to the smallest ones.[19] A formulation of the VMS approach for unstructured grids and the mixed finite-volume/finite-difference scheme, used in the present work, was provided by Koobus and Farhat.[22]

Another major difficulty for the success of LES for the simulation of complex flows is the fact that the cost of LES increases as the flow Reynolds number is increased. Indeed, the grid has to be fine enough to resolve a significant part of the turbulent scales, and this becomes particularly critical in the near-wall regions. A new class of models has recently been proposed in the literature in which RANS and LES approaches are combined together in order to obtain simulations as accurate as in the LES case but at reasonable computational costs. Among the hybrid models described in the literature, the Detached Eddy Simulation (DES) has received the largest attention. This approach[41] is generally based on the Spalart-Allmaras RANS model modified in such a way that far from solid walls and with refined grids, the simulation switches to the LES mode with a one-equation SGS closure. Another hybrid approach has been recently proposed, the *Limited Numerical Scales* (LNS),[2] in which the blending parameter depends on the values of the eddy-viscosity given by a RANS model and of the SGS viscosity given by a LES closure. In practice, the minimum of the two eddy-viscosities is used. An example of validation of LNS for the simulation of bluff-body flows is given in.[8]

A major difficulty in combining a standard RANS model with a LES one is due to the fact that RANS does not naturally allow for fluctuations, due to its tendency to damp them and to "perpetuate itself", as explained in.[41] On the other hand, LES needs a significant level of fluctuations in order to model the flow accurately enough. The abrupt passage from a RANS region to a LES one may produce the

so-called "modeled stress depletion".[41] We proposed a new strategy for blending RANS and LES approaches in a hybrid model.[14,31] To this purpose, as in,[23] the flow variables are decomposed in a RANS part (i.e. the averaged flow field), a correction part that takes into account the turbulent large-scale fluctuations, and a third part made of the unresolved or SGS fluctuations. The basic idea is to solve the RANS equations in the whole computational domain and to correct the obtained averaged flow field by adding, where the grid is adequately refined, the remaining resolved fluctuations. We search here for a hybridization strategy in which the RANS and LES models are blended in the computational domain following a given criterion. To this aim, a blending function is introduced, θ, which smoothly varies between 0 and 1. The correction term which is added to the averaged flow field is thus damped by a factor $(1-\theta)$, obtaining a model which coincides with the RANS approach when $\theta = 1$ and recovers the LES approach in the limit of $\theta \to 0$. Following strictly these guidelines would imply that the two fields, RANS and LES correction, need to be computed separately. In this first paper, we explore a single field version and investigate several other ingredients of the proposed hybrid family. In particular, three different definitions of the blending function θ are proposed and will be examined in this paper. They are based on the ratios between (i) two eddy viscosities, (ii) two characteristic length scales and (iii) two characteristic time scales given by the RANS and the LES models, respectively. The RANS model used in the proposed hybrid approach is the standard $k-\varepsilon$ model[25] or a low-Reynolds version,[17] while for the LES part the Variational MultiScale approach (VMS) is adopted.[19] The proposed hybridization strategy permits a natural integration of the VMS concept, while this is not the case for other existing approaches, as LNS or DES.

The paper is organized as follows: the main numerical ingredients are summarized in Sec. 2 and, in particular, the discretization of the convective terms is described. The different approaches to turbulence, viz. LES, VMS-LES and the hybrid model, are briefly presented in Sec. 3. Applications to two different bluff-body flows are then presented in Sec. 4. As previously mentioned, bluff-body flows are a typical example of massively separated flows, for which RANS simulations usually encounter difficulties in giving accurate predictions. Conclusions are finally drawn in Sec. 5.

2 Numerics

We consider here Newtonian, compressible three-dimensional and time-dependent flows. The governing equations corresponding to the different approaches for turbulence modeling, described in Sec. 3, are discretized in space using a mixed finite-volume/finite-element method applied to unstructured tetrahedrizations. The adopted scheme is vertex centered, i.e. all degrees of freedom are located at the vertexes. P1 Galerkin finite elements are used to discretize the diffusive terms. A dual finite-volume grid is obtained by building a cell C_i around each vertex i. The convective fluxes are discretized in terms of fluxes through the common boundaries shared by neighboring cells.

The Roe scheme[36] represents the basic upwind component for the numerical evaluation of the convective fluxes $\mathcal{F}$:

$$\Phi^R\left(W_i,\ W_j,\ \vec{n}\right) = \frac{\mathcal{F}\left(W_i,\ \vec{n}\right) + \mathcal{F}\left(W_j,\ \vec{n}\right)}{2} - \gamma_s d^R\left(W_i,\ W_j,\ \vec{n}\right) \qquad (1)$$

$$d^R\left(W_i,\ W_j,\ \vec{n}\right) = \left|\mathcal{R}\left(W_i,\ W_j,\ \vec{n}\right)\right| \frac{W_j - W_i}{2} \tag{2}$$

in which W_i is the solution vector at the i-th node, $\vec{n}$ is the normal to the cell boundary and $\mathcal{R}$ is the Roe Matrix. The parameter γ_s multiplies the upwind part of the scheme and permits a direct control of the numerical viscosity, leading to a full upwind scheme for $\gamma_s = 1$ and to a centered scheme when $\gamma_s = 0$. The MUSCL linear reconstruction method ("Monotone Upwind Schemes for Conservation Laws"), introduced by Van Leer,[44] is employed to increase the order of accuracy of the Roe scheme. The basic idea is to express the Roe flux as a function of a reconstructed value of W at the boundary between the two cells centered respectively at nodes i and j: $\Phi^R\left(W_{ij},\ W_{ji},\ \vec{n}_{ij}\right)$. W_{ij} is extrapolated from the values of W at the nodes, i.e. $W_{ij} = W_i + \frac{1}{2}(\vec{\nabla}W)_{ij}.\vec{ij}$, in which:

$$\begin{aligned}(\vec{\nabla}W)_{ij}.\vec{ij} = \ & (1-\beta)(\vec{\nabla}W)^C_{ij}.\vec{ij} + \beta(\vec{\nabla}W)^U_{ij}.\vec{ij} \\ & +\xi_c\left[(\vec{\nabla}W)^U_{ij}.\vec{ij} - 2(\vec{\nabla}W)^C_{ij}.\vec{ij} + (\vec{\nabla}W)^D_{ij}.\vec{ij}\right] \\ & +\xi_d\left[(\vec{\nabla}W)_M.\vec{ij} - 2(\vec{\nabla}W)_i.\vec{ij} + (\vec{\nabla}W)_j.\vec{ij}\right]\end{aligned} \tag{3}$$

With reference to Fig. 1, $(\vec{\nabla}W)^U_{ij}$ is the gradient on the upwind tetrahedron T_{ij}, $(\vec{\nabla}W)^D_{ij}$ is the gradient on the downwind tetrahedron T_{ji}, $(\vec{\nabla}W)_i$ is the nodal gradient computed over the finite-volume cell around node i, $(\vec{\nabla}W)_j$ is the nodal gradient computed over the finite-volume cell around node j, $(\vec{\nabla}W)^C_{ij}$ is the centered gradient ($(\vec{\nabla}W)^C_{ij}.\vec{ij} = W_j - W_i$) and $(\vec{\nabla}W)_M$ is the gradient at the point M. This last gradient is computed by interpolation of the nodal gradient values at the nodes contained in the face opposite to i in the upwind tetrahedron T_{ij}. The reconstruction of W_{ji} is analogous.

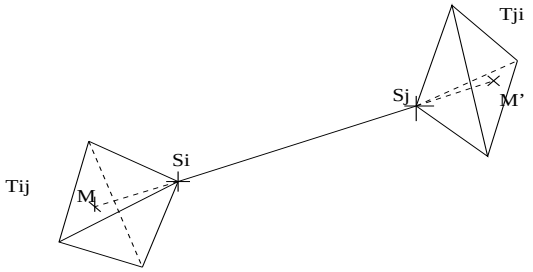

Figure 1: Sketch of points and elements involved in the computation of gradients

In choosing a particular set of free coefficients (β, ξ_c, ξ_d) in Eq. (3) attention has been dedicated to the dissipative properties of the resulting scheme which is a key point for its successful use in LES simulations. A first scheme has been proposed (V4),[7] characterized by $\beta = 1/3$, $\xi_c = \xi_d = 0$. Later, a second scheme has been proposed (V6),[6] characterized by $\beta = \frac{1}{3}$, $\xi_c = -\frac{1}{30}$ and $\xi_d = -\frac{2}{15}$.

The numerical dissipation in the schemes V4 and V6 is made of fourth- and sixth-order space derivatives, respectively, and, thus, it is concentrated on a narrow-band of the highest resolved frequencies. This is important in LES simulations to limit as far as possible the interactions between numerical and SGS dissipation, which could deteriorate the accuracy of the results.

Simulations can be advanced in time both with explicit or implicit schemes. In the first case, low-storage Runge-Kutta schemes are used. As for the implicit scheme, a second-order time-accurate backward difference scheme is adopted, which is based on a first-order approximation of the Jacobian matrix.[30]

A Turkel-type preconditioning term is introduced to avoid accuracy problems at low Mach numbers.[18] This kind of preconditioning is consistent in time and can thus be used also in time-dependent simulations.

More details on the numerical ingredients used in the present work can be found in Camarri et al.[6] and in Farhat et al.[11]

3 Approaches to turbulence

3.1 Large-eddy simulation

The LES approach consists in filtering in space the Navier-Stokes equations, in order to get rid of the high frequency fluctuations, and in simulating directly only the filtered flow. Due to the non-linearity of the problem, the filtered equations contain some unknown terms which represent the effect of the eliminated fluctuations on the filtered flow. These terms need to be modeled.

The filtered Navier-Stokes equations for compressible flows and in conservative form are considered. In our simulations, filtering is implicit, i.e. the numerical discretization of the equations is considered as a filter operator (grid filter).

In modeling the SGS terms resulting from filtering the Navier-Stokes equations, it is assumed that high Reynolds numbers flows are simulated, in which low compressibility effects are present in the SGS fluctuations. In addition, we assume that heat transfer and temperature gradients are moderate. Thus, the retained SGS term in the momentum equation is the classical SGS stress tensor:

$$M_{ij} \;=\; \overline{\rho u_i u_j} \;-\; \overline{\rho}\tilde{u}_i\tilde{u}_j \quad , \tag{4}$$

where the over-line denotes the grid filter and the tilde the density-weighted Favre filter ($\tilde{f} = \left(\overline{\rho f}\right) / \left(\overline{\rho}\right)$). The isotropic part of M_{ij} can be neglected under the assumption of low compressibility effects in the SGS fluctuations .[9] The deviatoric part, T_{ij}, is expressed by an eddy viscosity term:

$$T_{ij} = -2\mu_{\rm sgs}\left(\widetilde{S_{ij}} - \frac{1}{3}\widetilde{S_{kk}}\right) \quad , \tag{5}$$

$\widetilde{S_{ij}}$ being the resolved strain tensor, $\mu_{\rm sgs}$ the SGS viscosity.

In the total energy equation, the effect of the SGS fluctuations has been modeled by the introduction of a constant SGS Prandtl number to be *a priori* assigned:

$$Pr_{\rm sgs} = C_p\frac{\mu_{\rm sgs}}{K_{\rm sgs}} \tag{6}$$

where $K_{\rm sgs}$ is the SGS conductivity coefficient; it takes into account the diffusion of total energy caused by the SGS fluctuations and is added to the molecular conductivity coefficient. We refer to Camarri and Salvetti[4] and Camarri et al.[7] for a more detailed discussion of the simplifying assumptions leading to the adopted SGS modeling.

The different eddy-viscosity models used in the present work are briefly recalled in the following.

3.1.1 Smagorinsky model

In the Smagorinsky model the eddy viscosity is defined as follows:

$$\mu_{\mathrm{s}} = \overline{\rho}\,(C_{\mathrm{s}}\Delta)^2 \left|\widetilde{S}\right| \quad , \tag{7}$$

where Δ is the filter width and C_{s} is a constant that must be *a priori* assigned and $\left|\widetilde{S}\right| = \sqrt{2\widetilde{S_{ij}}\widetilde{S_{ij}}}$ (repeated indices imply summation). To complete the definition of the SGS viscosity, the grid filter width must be specified. Note that no reliable criteria exist to define the width of the filter corresponding to the adopted numerical discretization on unstructured grids. Nevertheless, the following expression has been employed here for each grid element j:

$$\Delta^{(j)} = Vol_j^{1/3} \tag{8}$$

where Vol_j is the volume of the $j-th$ grid element.

3.1.2 Dynamic model

The dynamic version of the Smagorinsky model has also been considered. The dynamic procedure proposed by Germano[16] is applied to the compressible Smagorinsky model described in the previous section. In this way, the coefficient that must be *a priori* assigned in the Smagorinsky model (C_{s}) is computed as a function of space at each time step. We have chosen to dynamically compute $(C_{\mathrm{s}}\Delta)^2$ instead of C_{s}^2, as in the classical dynamic model, in order to avoid the indetermination in the definition of the filter width. The test filter used here consists in P1-averaging the flow variables on all the elements having a given node as a vertex. The ratio $\widehat{\Delta}/\Delta$ ($\widehat{\Delta}$ being the test filter width), which is the only quantity to be *a priori* assigned in the dynamic model, is defined on each node as: $\widehat{\Delta}/\Delta = \sqrt[3]{N}$, where N is the number of elements having the node as a vertex. This is a consequence of the assumption that the size of the implicit filter scales as the cubic root of the element volume. A local smoothing is applied to avoid unphysical oscillations of $(C_{\mathrm{s}}\Delta)^2$. For more details on the implementation of this model see Camarri and Salvetti.[4]

3.1.3 Vreman's model

The eddy viscosity μ_v of the Vreman model[45] is defined by:

$$\mu_v = c(\frac{B_\beta}{\alpha_{ij}\alpha_{ij}})^{\frac{1}{2}} \tag{9}$$

with

$$\alpha_{ij} = \partial\tilde{u}_j/\partial x_i$$

$$\beta_{ij} = \Delta^2\alpha_{mi}\alpha_{mj}$$

$$B_\beta = \beta_{11}\beta_{22} - \beta_{12}^2 + \beta_{11}\beta_{33} - \beta_{13}^2 + \beta_{22}\beta_{33} - \beta_{23}^2$$

The constant $c \approx 2.5C_s^2$ where C_s denotes the Smagorinsky constant. The filter width Δ has been defined as done for the Smagorkinsky model.

3.1.4 WALE model

The Wall-Adapting Local Eddy -Viscosity (WALE) SGS model has been proposed by Nicoud and Ducros.[32] The eddy-viscosity term μ_w of the model is defined by:

$$\mu_w = C_w \Delta^2 \frac{(\overline{S_{ij}}^d \overline{S_{ij}}^d)^{\frac{3}{2}}}{(S_{ij}S_{ij})^{\frac{5}{2}} + (\overline{S_{ij}}^d \overline{S_{ij}}^d)^{\frac{5}{4}}} \tag{10}$$

with

$$\overline{S_{ij}}^d = \frac{1}{2}(\overline{g_{ij}}^2 + \overline{g_{ji}}^2) - \frac{1}{3}\delta_{ij}/\overline{g_{kk}}^2$$

being the symmetric part of the tensor $\overline{g_{ij}}^2 = \overline{g_{ik}g_{kj}}$, where $\overline{g_{ij}} = \partial \tilde{u}_i/\partial x_j$. The constant C_w is set to 0.1.

3.2 Variational multiscale LES

In the Variational MultiScale approach for Large Eddy Simulation (VMS-LES) the flow variables are decomposed as follows:

$$W = \underbrace{\overline{W}}_{LRS} + \underbrace{W'}_{SRS} + W^{SGS} \tag{11}$$

where $\overline{W}$ are the large resolved scales (LRS), W' are the small resolved scales (SRS) and W^{SGS} are the unresolved scales. This decomposition is obtained by projection in the LRS and SRS spaces respectively. In the present study, we follow the VMS approach proposed by Koobus and Farhat[22] for the simulation of compressible turbulent flows through a finite volume/finite element discretization on unstructured tetrahedral grids. Let ψ_l be the N finite-volume basis functions and ϕ_l the N finite-element basis functions associated to the used grid, in order to obtain the VMS flow decomposition in Eq. (11), the finite dimensional spaces $\mathcal{V}_{FV}$ and $\mathcal{V}_{FE}$, respectively spanned by ψ_l and ϕ_l, can be in turn decomposed as follows:[22]

$$\mathcal{V}_{FV} = \overline{\mathcal{V}}_{FV} \bigoplus \mathcal{V}'_{FV} \; ; \quad \mathcal{V}_{FE} = \overline{\mathcal{V}}_{FE} \bigoplus \mathcal{V}'_{FE} \tag{12}$$

in which $\bigoplus$ denotes the direct sum and $\overline{\mathcal{V}}_{FV}$ and $\mathcal{V}'_{FV}$ are the finite volume spaces associated to the largest and smallest resolved scales, spanned by the basis functions $\overline{\psi_l}$ and ψ'_l; $\overline{\mathcal{V}}_{FE}$ and $\mathcal{V}'_{FE}$ are the finite element analogous. A projector operator P in the LRS space is defined by spatial average on macro cells in the following way:[22]

$$\overline{\boldsymbol{W}} = P(\boldsymbol{W}) = \sum_k \underbrace{\left(\frac{Vol(C_k)}{\sum_{j \epsilon I_k} Vol(C_j)} \sum_{j \epsilon I_k} \psi_j \right)}_{\overline{\psi}_k} \boldsymbol{W}_k \tag{13}$$

for the convective terms, discretized by finite volumes, and:

$$\overline{\boldsymbol{W}} = P(\boldsymbol{W}) = \sum_k \underbrace{\left(\frac{Vol(C_k)}{\sum_{j \epsilon I_k} Vol(C_j)} \sum_{j \epsilon I_k} \phi_j \right)}_{\overline{\phi}_k} \boldsymbol{W}_k \tag{14}$$

for the diffusive terms, discretized by finite elements. In both Eqs. (13) and (14), $I_k = \{j / C_j \in C_{m(k)}\}$, $C_{m(k)}$ being the macro-cell containing the cell C_k. The macro-cells are obtained by a process known as agglomeration.[24] The basis functions for the SRS space are clearly obtained as follows: $\psi'_l = \psi_l - \overline{\psi}_l$ and $\phi'_l = \phi_l - \overline{\phi}_l$.

A key feature of the VMS-LES approach is that the modeled influence of the unresolved scales on large resolved ones is set to zero, and so the SGS model is added only to the smallest resolved scales (which models the dissipative effect of the unresolved scales on small resolved ones). Thus, let τ_{LES} be the closure term given by one of the SGS models described in Sec. 3.1, it is computed as a function of the smallest resolved scales, i.e.$\tau_{LES}(W')$, and the Galerkin projection of the corresponding term in the governing equations is given by: $(\tau_{LES}(W'), \phi'_l)$, where $(\cdot, \cdot)$ denotes the L^2 scalar product.

More details about this VMS-LES methodology can be found in Koobus and Farhat,[22] Farhat et al.[10] and Ouvrard et al.[34]

3.3 Hybrid RANS/LES coupling

As in Labourasse and Sagaut,[23] the following decomposition of the flow variables is adopted:

$$W = \underbrace{< W >}_{RANS} + \underbrace{W^c}_{correction} + W^{SGS}$$

where $< W >$ are the RANS flow variables, obtained by applying an averaging operator to the Navier-Stokes equations, W^c are the remaining resolved fluctuations (i.e. $< W > + W^c$ are the flow variables in LES) and W^{SGS} are the unresolved or SGS fluctuations.

If we write the Navier-Stokes equations in the following compact conservative form:

$$\frac{\partial W}{\partial t} + \nabla \cdot F(W) = 0$$

in which F represents both the viscous and the convective fluxes, for the averaged flow $\langle W \rangle$ we get:

$$\frac{\partial \langle W \rangle}{\partial t} + \nabla \cdot F(\langle W \rangle) = -\tau^{RANS}(\langle W \rangle) \tag{15}$$

where $\tau^{RANS}(\langle W \rangle)$ is the closure term given by a RANS turbulence model.

As well known, by applying a filtering operator to the Navier-Stokes equations, the LES equations are obtained, which can be written as follows:

$$\frac{\partial \langle W \rangle + W^c}{\partial t} + \nabla \cdot F(\langle W \rangle + W^c) = -\tau^{LES}(\langle W \rangle + W^c) \tag{16}$$

where τ^{LES} is the SGS term.

An equation for the resolved fluctuations W^c can thus be derived (see also[23]):

$$\frac{\partial W^c}{\partial t} + \nabla \cdot F(\langle W \rangle + W^c) \; - \; \nabla \cdot F(\langle W \rangle) = \tau^{RANS}(\langle W \rangle) - \tau^{LES}(\langle W \rangle + W^c) \quad (17)$$

The basic idea of the proposed hybrid model is to solve Eq. (15) in the whole domain and to correct the obtained averaged flow by adding the remaining resolved fluctuations (computed through Eq. (17)), wherever the grid resolution is adequate for a LES. To identify the regions where the additional fluctuations must be computed, we introduce a *blending function*, θ, smoothly varying between 0 and 1. When $\theta = 1$, no correction to $\langle W \rangle$ is computed and, thus, the RANS approach is recovered. Conversely, wherever $\theta < 1$, additional resolved fluctuations are computed; in the limit of $\theta \to 0$ we want to recover a full LES approach. Thus, the following equation is used here for the correction term:

$$\begin{aligned} &\frac{\partial W^c}{\partial t} \; + \; \nabla \cdot F(\langle W \rangle + W^c) \; - \; \nabla \cdot F(\langle W \rangle) = \\ &(1-\theta)\left[\tau^{RANS}(\langle W \rangle) - \tau^{LES}(\langle W \rangle + W^c)\right] \end{aligned} \quad (18)$$

Note that for $\theta \to 1$ the RANS limit is actually recovered; indeed, for $\theta = 1$ the right-hand side of Eq. (18) vanishes and, hence, a trivial solution is $W^c = 0$. As required, for $\theta = 0$ Eq. (18) becomes identical to Eq. (17) and the remaining resolved fluctuations are added to the averaged flow; the model, thus, works in LES mode. For θ going from 1 to 0, i.e. when, following the definition of the blending function (see Sec. 3.3.2), the grid resolution is intermediate between one adequate for RANS and one adequate for LES, the righthandside term in Eq. (18) is damped through multiplication by $(1-\theta)$. Although it could seem rather arbitrary from a physical point of view, this is aimed to obtain a smooth transition between RANS and LES. More specifically, we wish to obtain a progressive addition of fluctuations when the grid resolution increases and the model switches from the RANS to the LES mode.

Summarizing, the ingredients of the proposed approach are: a RANS closure model, a SGS model for LES and the definition of the blending function.

3.3.1 RANS and LES closures

For the LES mode, we wish to recover the variational multiscale approach described in Sec. 3.2. Thus, the Galerkin projection of Eqs. (15) and (18) for the computation of $\langle W \rangle$ and of the additional fluctuations in the proposed hybrid model become respectively:

$$\begin{aligned} &\left(\frac{\partial \langle W \rangle}{\partial t}, \psi_l\right) + (\nabla \cdot F_c(\langle W \rangle), \psi_l) + (\nabla \cdot F_v(\langle W \rangle), \phi_l) = \\ &-\left(\tau^{RANS}(\langle W \rangle), \phi_l\right) \quad l = 1, N \end{aligned} \quad (19)$$

$$\begin{aligned} &\left(\frac{\partial W^c}{\partial t}, \psi_l\right) + (\nabla \cdot F_c(\langle W \rangle + W^c), \psi_l) - (\nabla \cdot F_c(\langle W \rangle), \psi_l) + \\ &(\nabla \cdot F_v(W^c), \phi_l) = (1-\theta)\left[\left(\tau^{RANS}(\langle W \rangle), \phi_l\right) - \left(\tau^{LES}(W'), \phi_l'\right)\right] \quad l = 1, N \end{aligned} \quad (20)$$

where $\tau^{LES}(W')$ is given by one of the SGS closures described in Sec. 3.1.

As far the closure of the RANS equations is concerned, the standard $k-\varepsilon$ model[25] is used, in which the Reynolds stress tensor is modeled by introducing a turbulent eddy-viscosity μ_t, defined as a function of the turbulent kinetic energy k and of the turbulent dissipation rate of energy, ε, as follows:

$$\mu_t = C_\mu \rho \frac{k^2}{\varepsilon} \tag{21}$$

where C_μ is a model parameter, set here equal to the classical value of 0.09 and k and ε are obtained from the corresponding modeled transport equations (see Ref.[25]). The Low Reynolds $k-\varepsilon$ model proposed in[17] is also considered. The Reynolds stress tensor has the same form of that used in the standard $k-\varepsilon$ model but here the turbulent eddy-viscosity μ_t given by Eq. (21) is multiplied by a damping function f_μ, and k and ε are determined by ad-hoc modeled transport equations.[17]

3.3.2 Definition of the blending function and simplified model

As a possible choice for θ, the following function is used in the present study:

$$\theta = F(\xi) = tanh(\xi^2) \tag{22}$$

where ξ is the *blending parameter*, which should indicate whether the grid resolution is fine enough to resolve a significant part of the turbulence fluctuations, i.e. to obtain a LES-like simulation. The choice of the *blending parameter* is clearly a key point for the definition of the present hybrid model. In the present study, different options are proposed and investigated, namely: the ratio between the eddy viscosities given by the LES and the RANS closures, $\xi_{VR} = \mu_s/\mu_t$, which is also used as a blending parameter in LNS,[2] $\xi_{LR} = \Delta/l_{RANS}$, l_{RANS} being a typical length in the RANS approach, i.e. $l_{RANS} = k^{3/2}\epsilon^{-1}$ and, finally, $\xi_{TR} = t_{LES}/t_{RANS}$, t_{LES} and t_{RANS} being characteristic times of the LES and RANS approaches respectively, $t_{LES} = (S_{ij}S_{ij})^{-1/2}$ and $t_{RANS} = k\epsilon^{-1}$.

To avoid the solution of two different systems of PDEs and the consequent increase of required computational resources, Eqs. (19) and (20) can be recast together as:

$$\begin{aligned} &\left(\frac{\partial W}{\partial t}, \psi_l\right) + (\nabla \cdot F_c(W), \psi_l) + (\nabla \cdot F_v(W), \phi_l) = \\ &-\theta \left(\tau^{RANS}(\langle W \rangle), \phi_l \right) - (1-\theta) \left(\tau^{LES}(W'), \phi_l' \right) \quad l = 1, N \end{aligned} \tag{23}$$

Clearly, if only Eq. (23) is solved, $\langle W \rangle$ is not available at each time step. Two different options are possible: either to use an approximation of $\langle W \rangle$ obtained by averaging and smoothing of W, in the spirit of VMS, or to simply use in Eq. (23) $\tau^{RANS}(W)$. The second option is adopted here as a first approximation.

4 Applications

4.1 Flow around a square cylinder

The flow around a square cylinder of infinite length is considered, at a Reynolds number, based on the cylinder side length and on the freestream velocity, equal to 22000. A Cartesian frame of reference is considered, with the origin coinciding with the gravity center of the square section and the x and z axes oriented in the streamwise and spanwise directions, respectively.

LES and experiments	C_l'	$\overline{C_d}$	C_d'	l_r
S_V4_G05_GR1	0.79	1.84	0.10	1.45
S_V6_G05_GR1	0.84	1.89	0.09	1.41
S_V6_G05_GR2	1.10	2.2	0.18	1.15
D_V4_G05_GR1	0.91	2.03	0.12	1.24
D_V6_G05_GR1	0.94	2.06	0.10	1.33
D_V4_G10_GR1	0.84	1.94	0.09	1.53
D_V6_G10_GR1	0.86	2.02	0.09	1.47
D_V6_G05_GR2	1.09	2.10	0.15	1.15
V_V6_G20_GR2	1.08	2.10	0.18	1.4
Rodi et al.[35]	[0.38,1.79]	[1.66,2.77]	[0.10,0.27]	[0.89,2.96]
Sohankar et al.[40] and Fureby et al.[13]	[1.23,1.54]	[2.0,2.32]	[0.16,0.20]	[1.29-1.34]
Lyn et al.[28,29]	-	2.1	-	1.4
Bearman et al.[3]	1.2	2.28	-	-
Norberg[33]	-	2.16	-	-
Luo et al.[27]	1.21	2.21	0.18	-

Table 1: Bulk coefficients; comparison with experimental data and with other simulations in the literature. $\overline{C_d}$ is the mean drag coefficient, C_d' and C_l' are the r.m.s. of the drag and lift coefficients and l_r is the length of the mean recirculation bubble. The name of the simulations is composed in this way: the first part indicates the turbulence model ("S" stands for the Smagorinsky model, "D" for the Dynamic one and "V" for the VMS-LES with the Smagorinsky closure), the second indicates the scheme adopted for the convective fluxes, the third indicates the value of the parameter γ_s (in hundredth), the fourth indicates the adopted grid.

4.1.1 LES simulations

In the LES simulations that will be described in the following, a computational domain is adopted with dimensions $L_i/D = 5$, $L_o/D = 10$, $L_s/D = 4$ and $H/D = 7$, where D is the side length of the square section, L_i and L_o are the distances between the cylinder center of gravity and the inflow and outflow boundaries, respectively, L_s is the width of the domain in the spanwise direction and H is the distance between the cylinder axis and the domain boundaries in the y direction.

Boundary conditions based on Steger-Warming decomposition[42] are used at the inflow and at the outflow surfaces. On the side surfaces free-slip is imposed and the flow is assumed to be periodic in the spanwise direction. Approximate boundary conditions based on the Reichardt wall-law are used on the cylinder surface (see Camarri et al.[7]and Camarri and Salvetti[5]).

The results shown in the following have been obtained on two grids: the first (GR1) of about 10^5 nodes and 6×10^5 elements, the second (GR2), more refined, having approximately $2{\times}10^5$ nodes and $1.1{\times}10^6$ elements. The average distance of the first layer of nodes from the cylinder surface is $6 \times 10^{-2}D$ for GR1 and $4.5 \times 10^{-2}D$ for GR2. For both grids, approximately 32 nodes are located in the spanwise direction within the wake region.

The main bulk coefficients obtained in the LES simulations, with the Smagorinsky model, the dynamic model and in the VMS-LES simulations with the Smagorinsky closure, are presented in Tab. 1, together with results from other LES simulations[13,35,40] and experimental data.[3,27–29,33]

As shown in Tab. 1, the results obtained with the V4 scheme are sensitive to the choice of the parameter γ_s and, when this is tuned close to the minimum value com-

patible with numerical stability, the LES simulations are of sufficient predicivity. Nevertheless, as shown in Camarri et al.,[7] the numerical viscosity gives a contribution to the fluxes which is more important than the one given by the dynamic model, while the LES model contribution is dominant when the more dissipative Smagorinsky model is used. This drawback, as well as the need of a fine tuning of the parameter γ_s have been overcome with the V6 scheme. Indeed, the results in Tab. 1 show a reduced sensitivity of the predicted bulk coefficients to γ_s when V6 is used. Moreover, the accuracy of the results is improved, especially concerning the unsteady part of the flow field. Indeed, the values of the r.m.s. of the force coefficients is generally higher with V6 (see Tab.1). Moreover, independently of the SGS model, in the simulations with V6 a larger energy content than with V4 is found in all the resolved frequencies, and especially in the highest ones, as shown for instance by the Fourier spectra in Figure 2. This is well shown, for instance, in Fig. 2 where the Fourier energy spectra of the velocity signals measured in a point in the wake in D_V4_G05_GR1 and D_V6_G05_GR1 are compared. The mean con-

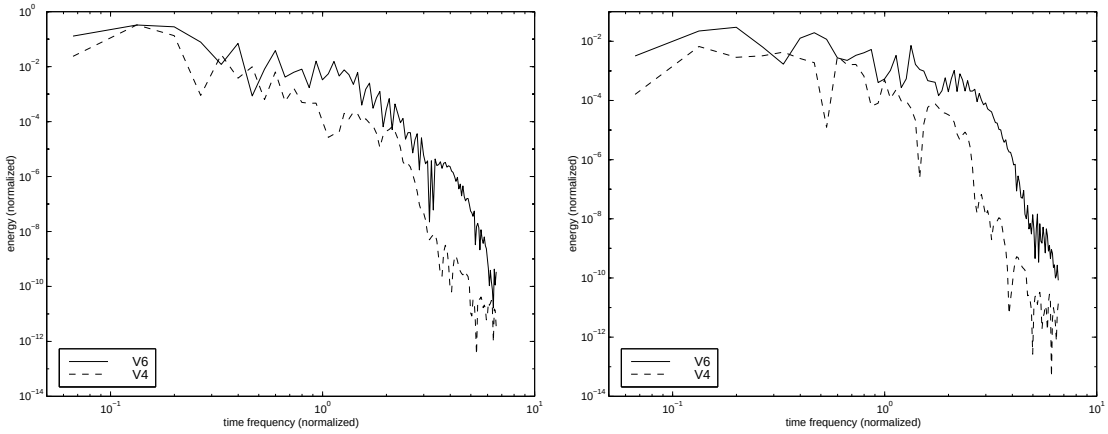

(a) (b)

Figure 2: Simulations D_V4_G05_GR1 and D_V6_G05_GR. Fourier energy spectra of the velocity components recorded at $x = 3$, $y = 0.5$ and $z = 0$. a) Transverse velocity v; b) spanwise velocity w.

vection velocity in the considered points within the wake is large enough to justify the Taylor hypothesis of frozen turbulence which allows us to assume that high time frequencies correspond to small scale in space; thus, one might conclude that small scales are less damped by the V6 scheme.

As regards the SGS modeling interaction with the adopted numerical scheme, Tab. 1 shows that the qualitative variations of the bulk coefficients with the SGS model are the same for V4 and V6, i.e. the dynamic model generally improves predictions with respect to the Smagorinsky model. However, quantitatively, the sensitivity to SGS modeling of the results obtained with V6 is lower than with V4. This is particularly evident from the comparison of the Reynolds stresses, not shown here for the sake of brevity, and this is related to the larger energy content at the small scales obtained with V6; see Camarri et al.[6] for a more detailed discussion.

The grid refinement improves results particularly when the Smagorinsky model is used, while the simulations with the dynamic model give acceptable results also on the grid GR1. However the dynamic model is definitely more CPU-demanding than

the Smagorinsky one, due to the explicit filtering required in the dynamic procedure, which is highly computationally demanding on unstructured grids. As an example, when the dynamic model is used instead of the Smagorinsky one with the V4 scheme and an explicit time advancing, an increase of about 180% CPU time per time step is measured.

The best compromise between accuracy and computational costs has been obtained by the adoption of the VMS-LES model, properly formulated for our numerics. Indeed, Tab. 1 shows that the level of accuracy of the VMS-LES model, with the Smagorinsky SGS closure, is comparable with that of the dynamic model. At the same time, its computational cost is only slightly larger than that of the Smagorinsky model. Finally, note that the problems of numerical stability typically encountered with the dynamic model, unless ad-hoc smoothing or clipping of the model coefficient values is carried out, are obviously not present in the VMS approach. A more detailed discussion of the results obtained with the VMS-LES model can be found in Ref.[22]

4.1.2 Hybrid RANS/LES simulations

In the simulations described in the following, a computational domain is adopted which differs from the one used in the LES simulations only for the width in the spanwise direction, which is $L_s/D = 9.75$. The spanwise extension of the new domain is the same as that of the water tunnel used in the experiments of Lyn et al.[28] and Lyn and Rodi.[29] Thus, in the second and third sets of simulations, slip conditions have been applied also in the spanwise direction instead of periodic ones. The remaining boundary conditions are unchanged.

The results shown in the following have been obtained on two grids: the first (GR3) of about 8.3×10^4 nodes and 4.75×10^5 elements, the second (GR4) having approximately 3.5×10^4 nodes and 1.9×10^5 elements. Note that both grids are significantly coarser than those typically used in the literature for LES, but also for DES simulations, of this flow. We chose to use coarse grids in order to have the model working in hybrid mode, since both the LNS and the proposed approach tend to LES if the grid is adequately refined (see Camarri et al.[8]). Following the LNS work in Camarri et al.,[8] the numerical parameter γ_s, which controls the amount of numerical viscosity introduced in the simulation, has been set equal to 0.1 for GR3 and 0.5 for GR4, i.e. the minimum value required to obtain stable simulations.

The simulations have been implicitly advanced in time, with a maximum CFL number ranging from 10 to 20. In Camarri et al.[8]), it was shown that no significant information is lost in time provided that CFL$\leq$ 25.

For both grids, the computations have been carried out using the LNS model and the new proposed hybrid model (*Continuous Correction Hybrid Model*, CCHM) with different definitions of the blending parameter. The parameters characterizing the different simulations are summarized in Tab. 2. In the LNS calculations the RANS and LES closure were respectively given by the Smagorinsky and the standard $k-\varepsilon$ models respectively, while in the CCHM simulations the VMS-LES approach together with the Smagorinsky model and the low-Reynolds version of the $k-\varepsilon$ model were used (see Sec. 3). Tab. 2 also shows the main bulk flow parameters, including the vortex shedding frequency, St, which is adimensionalized with D and the free-stream velocity. Let us analyze, first, the sensitivity to grid refinement by

Simulations	Grid	Model	ξ	$\overline{C_d}$	C'_d	C'_l	St	l_r
LNS1	GR3	LNS	–	2.11	0.116	0.654	0.131	1.15
LNS2	GR4	LNS	–	2.07	0.087	0.685	0.13	1.19
CCHM1	GR3	CCHM	VR	1.95	0.107	0.81	0.13	1.37
CCHM2	GR3	CCHM	TR	2.01	0.117	0.792	0.131	1.16
CCHM3	GR4	CCHM	VR	2.01	0.074	0.58	0.129	1.1
CCHM4	GR4	CCHM	TR	2.01	0.071	0.6	0.131	1.21
CCHM5	GR4	CCHM	LR	2.01	0.083	0.63	0.128	1.1
LES[8]	GR4	Smagorinsky	–	1.71	0.02	0.31	0.137	2.8
RANS[8]	GR4	$k-\varepsilon$	–	1.53	0.01	0.20	0.117	2.38
DES[38]	–	DES	–	2.42-2.57	0.28-0.68	1.36-1.55	0.09-0.13	1.16-1.37
DES[26]	–	DES	–	2.18	–	–	0.134	0.81
Exp.[3]	–	–	–	2.28	–	1.2	0.13	–
Exp.[29]	–	–	–	2.1	–	–	0.132	1.4

Table 2: Simulation parameters and main bulk flow quantities for the square cylinder test case. VR stands for viscosity ratio, TR for time ratio and LR for length ratio.

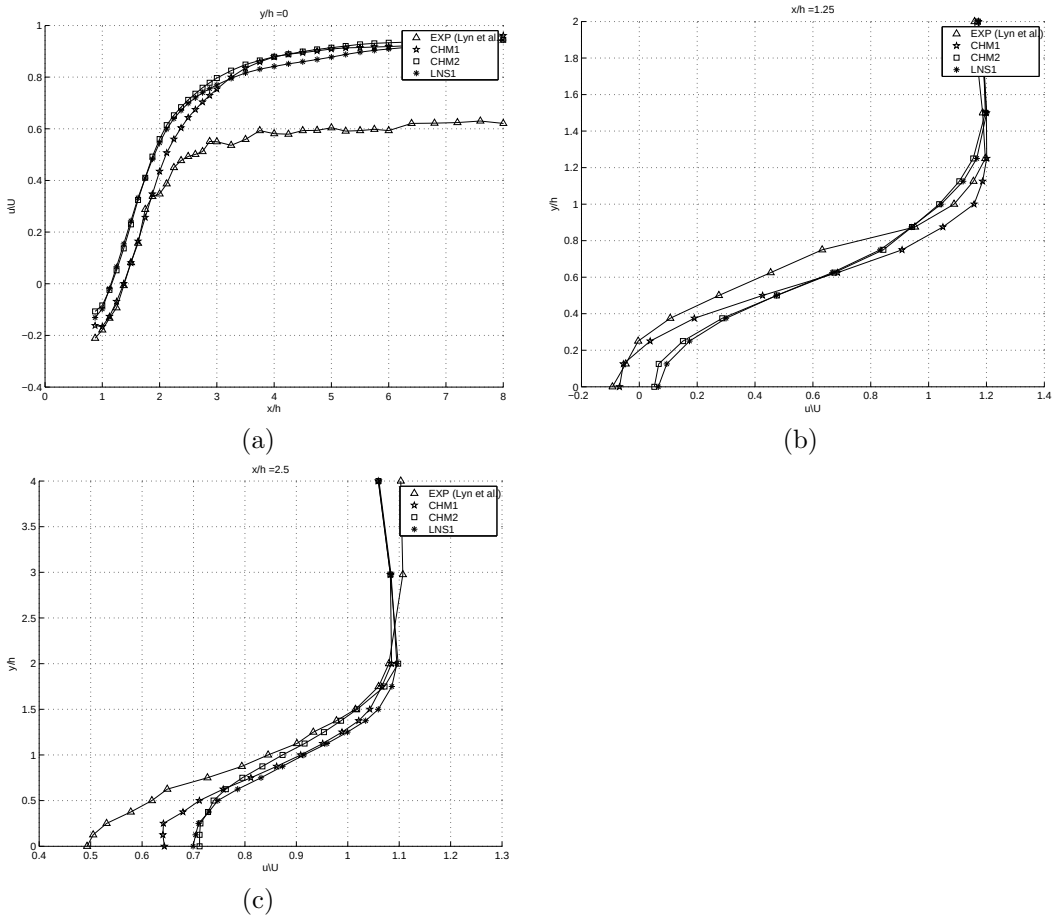

Figure 3: Mean horizontal-velocity profiles for CCHM1, CCHM2 and LNS1 plane y/L=0 (a), x/L=1.25 (b), x/L=2.5 (c)

comparing CCHM1 with CCHM3 and CCHM2 with CCHM4. The most significant differences are in the force r.m.s., and, in particular, larger fluctuations are found for the more refined grid. This is consistent with the basic idea of the proposed model, i.e. to progressively add more fluctuations as the grid resolution increases. As for the definition of the blending parameter, its effect on the computed flow bulk parameters is rather small, the most sensitive quantity being l_r with a variation of 15% between CCHM1 and CCHM2. The overall agreement with the experimental values is fairly good, especially reminding the very coarse grid resolution of the present simulations. Note that, as reported in Tab. 2, LES and RANS simulations carried out on the same grid give inaccurate predictions. As previously mentioned, the results of DES reported in Tab. 2 are obtained with significantly finer grid resolution. An example of predictions of velocity profiles on grid GR3 is given in Fig. 3, which shows the streamwise velocity profiles along the centerline (Fig. 3 (a)) and in the lateral direction at two different locations in the wake (x/h=1.25 in Fig. 3 (b) and x/h=2.5 in Fig. 3 (c)). It can be seen that the differences between the models are small. The overall agreement with the experiments may be considered satisfactory, except for the much higher recovery velocity obtained in all simulations with respect to the experiments. This is, however, a discrepancy observed in almost all the previous simulations in the literature and is discussed, for instance, in Camarri et al.[7] Finally, the behavior of the proposed hybrid model in the field is very similar for all the considered definitions of the blending parameter and grids. In particular, the model works in the LES mode in the wake, in the RANS mode in the shear-layers detaching from the cylinder corners, while damped fluctuations are added in a layer at the wake edges. As an example, Fig. 4 shows the instantaneous isocontours of the spanwise vorticity obtained in the simulation CCHM5, to which the isolines of the blending function $\theta = 0.4$ and $\theta = 0.9$ are superimposed.

4.2 Hybrid simulations of the flow around a circular cylinder

The CCHM approach has also been applied to the simulation of the flow around a circular cylinder at $Re = 140000$ (based on the far-field velocity and the cylinder diameter). The domain dimensions are $L_i/D = 5$, $L_o/D = 15$, $H/D = 7$ and $L_s/D = 2$ (the symbols are the same as in Sec. 4.1). Two grids have been used, the first one (GR1) has 4.6×10^5 nodes, while the second one has (GR2) 1.4×10^6 nodes. Both grids are composed of a structured part around the cylinder boundary and a unstructured part in the rest of the domain. The inflow conditions are the same as in the DES simulations of Travin et al.[43] In particular, the flow is assumed to be highly turbulent by setting the inflow value of eddy-viscosity to about 5 times the molecular viscosity as in the DES simulation of Travin et al.[43] This setting corresponds to a free-stream turbulence level $\overline{u'^2}/U_0$ (where u' is the inlet velocity fluctuation and U_0 is the free-stream mean velocity) of the order of 4%. As discussed also by Travin et al.,[43] the effect of such a high level of free-stream turbulence is to make the boundary layer almost entirely turbulent also at the relatively moderate considered Reynolds number. The boundary treatment is the same as for the hybrid simulations of the square cylinder flow test-case, except that the flow is assumed to be periodic in the spanwise direction in order to simulate a cylinder of infinite spanwise length. The RANS model is that based on the Low-Reynolds approach,[17]

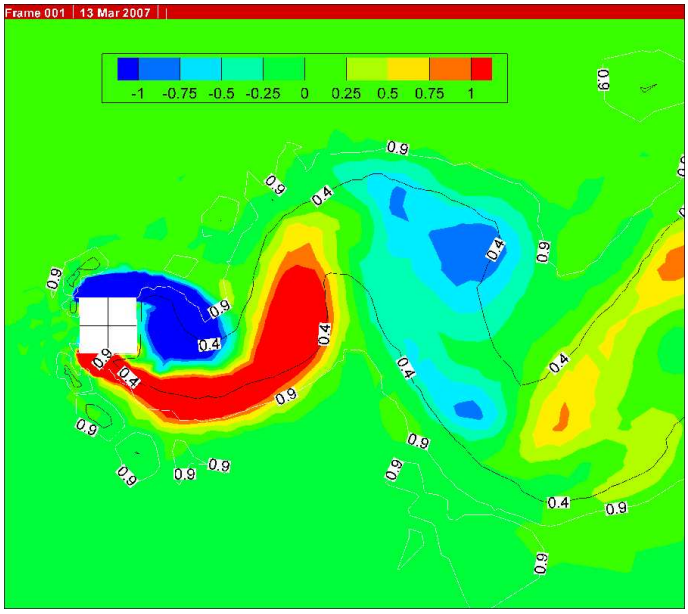

Figure 4: Plot of the instantaneous isocontours of the spanwise vorticity for the simulation CCHM5. The isolines $\theta = 0.4$ (black) and $\theta = 0.9$ (white) are also reported.

briefly described in Sec. 3.3.1. The LES closure is based on the VMS approach (see Sec.3.2). The SGS models used in the simulations are those described in Sec.3.1. The V6 scheme has been used and the numerical parameter γ_s, which controls the amount of numerical viscosity introduced in the simulation, has been set equal to 0.2. The main parameters characterizing the simulations carried out with the CCHM are summarized in Tab. 3. The main flow bulk parameters obtained in

Simulation	Blending parameter	Grid	LES-SGS model
CCHM1	VR	GR1	Smagorinsky
CCHM2	LR	GR1	Smagorinsky
CCHM3	LR	GR2	Smagorinsky
CCHM4	LR	GR1	Vreman
CCHM5	LR	GR1	Wale

Table 3: Simulation name and their main characteristics

the present simulations are summarized in Tab. 4, together with the results of DES simulations in the literature and some experimental data. Let us analyze, first, the sensitivity to the blending parameter, by comparing the results of the simulation CCHM1 and CCHM2. As for the square cylinder test-case, the results are practically insensitive to the definition of the blending parameter. Conversely, the grid refinement produced a decrease of $\bar{C}_d$ and a delay in the boundary layer separation (compare CCHM2 and CCHM3). However, note that, for unstructured grids, the refinement changes the local quality of the grid (in terms of homogeneity and regularity of the elements) and this may enhance the sensitivity of the results. The sensitivity to the VMS-LES closure model is also very low (compare CCHM2, CCHM4 and CCHM5). This very low sensitivity has been observed also in VMS-LES simulations of the same flow carried out at low Reynolds number (see the companion

Simulations	Re	$\overline{C_d}$	C_l'	St	l_r	θ_{sep}
CCHM1	1.4 10^5	0.62	0.083	0.30	1.20	108
CCHM2	1.4 10^5	0.62	0.083	0.30	1.19	108
CCHM3	1.4 10^5	0.54	0.065	0.33	1.13	115
CCHM4	1.4 10^5	0.65	0.077	0.28	1.14	109 (99)
CCHM5	1.4 10^5	0.66	0.094	0.28	1.24	109 (100)
DES[43]	1.4 10^5	0.57-0.65	0.08-0.1	0.28-0.31	1.1 -1.4	93-99
DES[26]	1.4 10^5	0.6-0.81	–	0.29-0.3	0.6-0.81	101-105
Exp.[20]	3.8 10^6	0.58	–	0.25	–	110
Exp.[1]	5 10^6	0.7	–	–	–	112
Exp.[37]	8 10^6	0.52	0.06	0.28	–	–

Table 4: Main bulk flow quantities for the circular cylinder test case. Same notations as in Tab. 2. θ_{sep} is the separation angle.

paper presented in this same conference[34]) and, thus, it seems more peculiar to the VMS-LES approach rather than to the hybrid model.

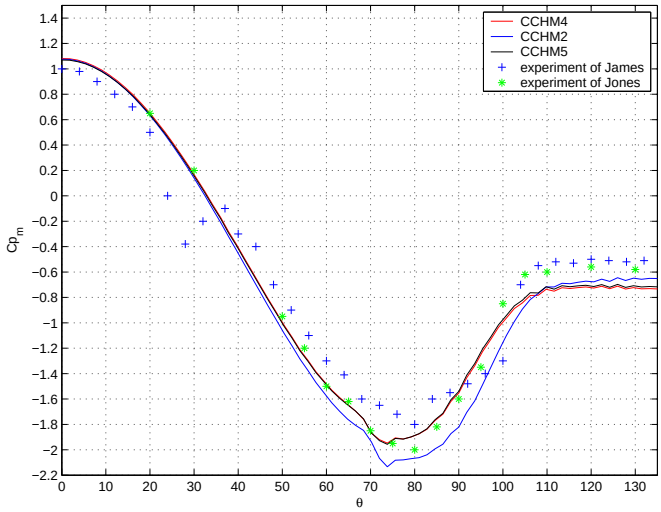

Figure 5: $\bar{C_p}$ on the cylinder surface compared to numerical and experimental results

The agreement with the DES results is fairly good. As for the comparison with the experiments, as also stated in Travin et al.,[43] since our simulations are characterized by a high level of turbulence intensity at the inflow, it makes sense to compare the results with experiments at higher Reynolds number, in which, although the level of turbulence intensity of the incoming flow is very low, the transition to turbulence of the boundary layer occurs upstream separation. The agreement with these high Re experiments is indeed fairly good, as shown in Tab. 4 and in Fig. 5. The behavior of the separation angle requires a brief discussion. There is a significant discrepancy between the values obtained in DES and the experimental ones. For our simulations, the values of θ_{sep} shown in Tab. 4 are estimated by considering the point at which the C_p distribution over the cylinder becomes nearly constant (see e.g. Fig. 5), as usually done in experimental studies. Indeed, the reported values are generally in better agreement with the experiments than those obtained by DES. However, if we estimate the separation angle from the streamlines of the average

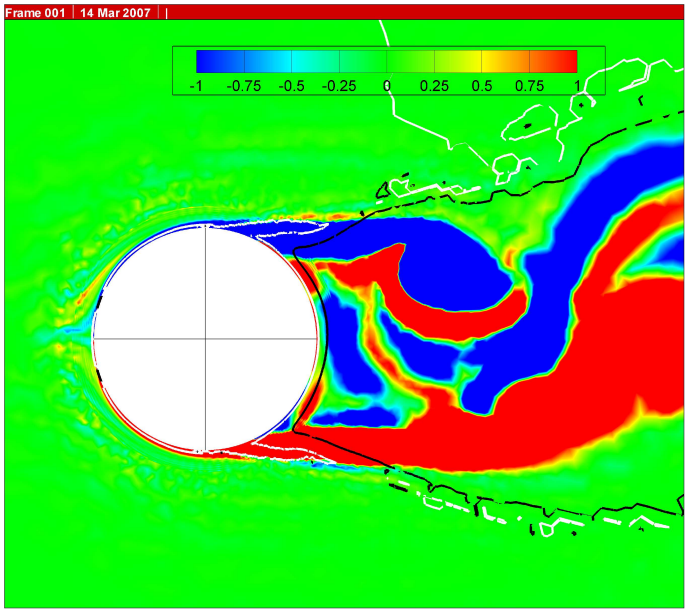

Figure 6: Instantaneous isocontours of spanwise vorticity (simulation CCHM2). The black and white lines are the isolines of the blending function $\theta = 0.1$ and $\theta = 0.9$.

or instantaneous velocity fields, significantly lower values are found (reported in parentheses in Tab. 4 for the simulations CCHM4 and CCHM5); these values are closer to those obtained by DES. Finally, the behavior of the hybridization strategy in the field is similar to that obtained for the square cylinder test case; indeed, the model works in RANS mode in the boundary layer and in the shear-layers detaching from the cylinder, while in the wake a full LES correction is recovered. This is shown, for instance, in Fig. 6, in which the instantaneous isocontours of spanwise vorticity obtained in the simulation CCHM2 are reported, to which the isolines of the blending function $\theta = 0.1$ and $\theta = 0.9$ are superimposed. As for the behavior with grid refinement, it is, at least qualitatively, correct. Indeed, the extension of the zone in the detaching shear-layers in which the model works in RANS mode decreases with grid refinement, as shown for instance in Figs. 7, reporting a zoom near the cylinder of the instantaneous isocontours of the blending function θ, obtained in the simulations CCHM2 and CCHM3.

5 Concluding remarks

The research activity carried out by our group towards the accurate numerical prediction of complex flows has been summarized here. Our starting point was a numerical solver for compressible flows on unstructured grids, through a mixed finite-element/finite-volume formulation, designed and validated for RANS simulations.

The first main action was to move to a LES approach to turbulence in order to deal with massively separated and highly unsteady and 3D flows for which the RANS approach encounter accuracy problems. This brought some issues to be tackled. First of all, the numerical method had to be adapted to the new turbulence treatment. The most critical point was, at least in our opinion, the possible negative

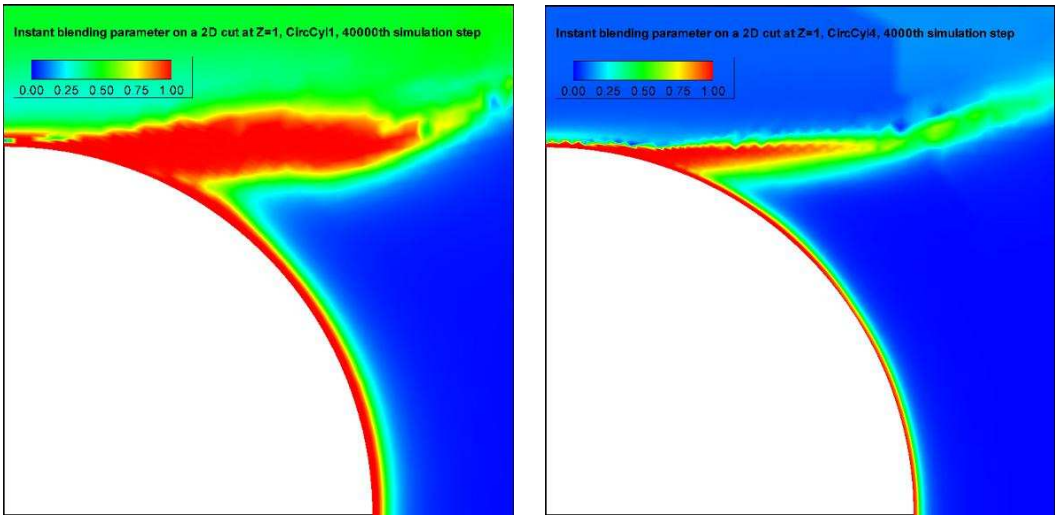

Figure 7: Instantaneous isocontours of the blending function θ. Simulations CCHM2 (a) and CCHM3 (b).

interaction between the LES closure model and the numerical viscosity, required for numerical stability of our co-located discretization. Our proposition was to keep a physically based closure model and to modify the MUSCL reconstruction in order to obtain a numerical viscosity proportional to high-order (4th or 6th order) spatial derivatives. In this way, the numerical dissipation is concentrated on a narrow band of the smallest resolved scales and thus its interaction with the SGS dissipation, usually proportional to second-order spatial derivatives, is reduced. Moreover, a coefficient was introduced to tune numerical dissipation to the smallest amount required to stabilize the simulation. This strategy was validated through the application to the large-eddy simulation of different types of flows. As an example, in this paper the results obtained for the flow around a square cylinder have been described.

As for SGS models, some difficulties due to the use of *classical* models on unstructured grids appeared. For instance, the dynamic version of the Smagorinsky model gave, as generally found in the literature, more accurate results than the Smagorinsky model, but resulted in a dramatic increase in the computational costs, much larger than that observed for structured grids. This led us to the use of the variational multiscale formulation, which was adapted to the present mixed finite-element/finite-volume discretization on unstructured grids. As also shown in the present paper, this approach gave results as accurate as LES with the dynamic model but at computational costs comparable with those of the Smagorinsky model.

Another critical issue for the use of LES for the simulation of flows at high Reynolds numbers is the near wall resolution. Indeed, the grid has to be fine enough to resolve a significant part of the turbulent scales, and this becomes particularly critical in the near-wall regions. This led to the so-called hybrid models, recently proposed in the literature, in which RANS and LES approaches are combined together in order to obtain simulations as accurate as in the LES case but at reasonable computational costs. A new strategy for blending RANS and LES has been described here which is based on a decomposition of the flow variables in a RANS part and a

correction part, which takes into account the resolved fluctuations. To identify the zones in which the correction must be computed and added to the RANS part, a blending function is introduced such that the model works in RANS mode where the grid is coarse and tends with continuity to LES as the grid refinement becomes adequate. For the closure of the LES part, the VMS approach has been integrated in the proposed hybridization strategy. As a first choice, we use here a simplified version of the model in which only one set of unknowns is computed. The proposed method has been applied to the hybrid simulations of the flows around two different bluff-bodies, viz. a square cylinder and a circular one. The results are promising, both for the accuracy of the prediction of the bulk flow parameters which is in good agreement with experimental data and the results of different simulations in the literature, as well as for the behavior of the blending function which shows a sensible distribution in the field. Moreover, the proposed approach shows a very low sensitivity to the choice of the blending parameter and to the closure model used for VMS-LES.

Acknowledgments

CINECA (Bologna, Italy) and CINES (Montpellier, France) are gratefully acknowledged for having provided the computational resources.

References

[1] E. Achenbach. Distribution of local pressure and skin friction around a circular cylinder in cross-flow up to Re= 5×10^6. *J. Fluid Mech.*, 34(4):625–639, 1968.

[2] P. Batten, U. Goldberg, and S. Chakravarthy. Interfacing statistical turbulence closures with large-eddy simulation. *AIAA Journal*, 42(3):485–492, 2004.

[3] P. W. Bearman and E. D. Obasaju. An experimental study of pressure fluctuations on fixed and oscillating square-section cylinders. *J. Fluid Mech.*, 119:297–321, 1982.

[4] S. Camarri and M. V. Salvetti. Towards the large-eddy simulation of complex engineering flows with unstructured grids. Technical Report RR-3844, INRIA, 1999.

[5] S. Camarri and M. V. Salvetti. On the approximate treatment of wall boundary conditions in large-eddy simulation. Technical Report ADIA 2002-3, Dep. Aerospace Engineering - University of Pisa, December 2002.

[6] S. Camarri, M. V. Salvetti, B. Koobus, and A. Dervieux. A low diffusion MUSCL scheme for LES on unstructured grids. *Computers and Fluids*, 33:1101–1129, 2004.

[7] S. Camarri, M.V. Salvetti, B. Koobus, and A. Dervieux. Large-eddy simulation of a bluff-body flow on unstructured grids. *Int. J. Num. Meth. Fluids*, 40:1431–1460, 2002.

[8] S. Camarri, M.V. Salvetti, B. Koobus, and A. Dervieux. Hybrid RANS/LES simulations of a bluff-body flow. *Wind & Structures*, 8:407–426, 2005.

[9] G. Erlebacher, M. Y. Hussaini, C. G. Speziale, and T. A. Zang. Toward the large-eddy simulation of compressible flows. *J. Fluid Mech.*, 238:155–185, 1992.

[10] C. Farhat, A. Kajasekharan, and B. Koobus. A dynamic variational multiscale method for large eddy simulations on unstructured meshes. *Computational Methods in Applied Mechanics and Engineering*, pages 1688–1691, 2005.

[11] C. Farhat, B. Koobus, and H. Tran. Simulation of vortex shedding dominated flows past rigid and flexible structures. In *Computational Methods for Fluid-Structure Interaction*, pages 1–30. Tapir, 1999.

[12] Grinstein F.F. and Fureby C. From canonical to complex flows: Recent progress on monotonically integrated les. *Computing in Science and Engineering*, 6(2):36–49, 2006.

[13] C. Fureby, G. Tabor, H. G. Weller, and A. D. Gosman. Large eddy simulation of the flow around a square prism. *AIAA Journal*, 38(3):442–452, 2000.

[14] Pagano G., Camarri S., Salvetti M.V., Koobus B., and Dervieux A. Strategies for rans/vms-les coupling. Technical Report RR-5954, INRIA, 2006.

[15] E. Garnier, P. Sagaut, P. Comte, and M. Deville. On the use of shock-capturing schemes for large-eddy simulation. *J. Comp. Phys*, 153:273–311, 1999.

[16] M. Germano, U. Piomelli, P. Moin, and W. Cabot. A dynamic subgrid-scale eddy viscosity model. *Phys. Fluids A*, 3(7):1760–1765, 1991.

[17] U. Goldberg, O. Peroomian, and S. Chakravarthy. A wall-distance-free $k-\varepsilon$ model with enhanced near-wall treatment. *Journal of Fluids Engineering*, 120:457–462, 1998.

[18] H. Guillard and C. Viozat. On the behaviour of upwind schemes in the low Mach number limit. *Computers and Fluids*, 28:63–86, 1999.

[19] T.J.R. Hughes, L. Mazzei, and K.E. Jansen. Large eddy simulation and the variational multiscale method. *Comput. Vis. Sci.*, 3:47–59, 2000.

[20] W.D. James, S.W. Paris, and G.V. Malcolm. Study of viscous cross flow effects on circular cylinders at high Reynolds numbers. *AIAA Journal*, 18:1066–1072, 1980.

[21] Mahesh k., Constantinescu G., and Moin P. A numerical method for large-eddy simulation in complex geometries. *J. Comp. Phys.*, 197(1):215–240, 2004.

[22] B. Koobus and C. Farhat. A variational multiscale method for the large eddy simulation of compressible turbulent flows on unstructured meshes-application to vortex shedding. *Comput. Methods Appl. Mech. Eng.*, 193:1367–1383, 2004.

[23] E. Labourasse and P. Sagaut. Reconstruction of turbulent fluctuations using a hybrid RANS/LES approach. *J. Comp. Phys.*, 182:301–336, 2002.

[24] M.H. Lallemand, H. Steve, and A. Dervieux. Unstructured multigridding by volume agglomeration: current status. *Comput. Fluids*, 21:397–433, 1992.

[25] B.E. Launder and D.B. Spalding. The numerical computation of turbulent flows. *Comp. Meth. Appl. Mech. and Eng.*, 3:269–289, 1979.

[26] S.-C. Lo, K.A. Hofmann, and J.-F. Dietiker. Numerical investigation of high Reynolds number flows over square and circular cylinder. *Journal of Thermophysics and Heat Transfer*, 19:72–80, 2005.

[27] S. C. Luo, MdG. Yazdani, Y. T. Chew, and T. S. Lee. Effects of incidence and afterbody shape on flow past bluff cylinders. *J. Ind. Aerodyn.*, 53:375–399, 1994.

[28] D. A. Lyn, S. Einav, W. Rodi, and J. H. Park. A laser-doppler velocimeter study of ensemble-averaged characteristics of the turbulent near wake of a square cylinder. *J. Fluid Mech.*, 304:285–319, 1995.

[29] D.A. Lyn and W. Rodi. The flapping shear layer formed by flow separation from the forward corner of a square cylinder. *J. Fluid Mech.*, 267:353–376, 1994.

[30] R. Martin and H. Guillard. A second-order defect correction scheme for unsteady problems. *Comput. and Fluids*, 25(1):9–27, 1996.

[31] Salvetti M.V., Koobus B., Camarri S., and Dervieux A. Simulation of bluff-body flows thorugh a hybrid rans/vms-les model. In *Proceedings of the IUTAM Symposium on Unsteady Separated Flows and their Control*, Corfu (Grece), June 18-22 2007.

[32] F. Nicoud and F. Ducros. Subgrid-scale stress modelling based on the square of the velocity gradient tensor. *Flow Turbulence and Combustion*, 62(3):183–200, 1999.

[33] C. Norberg. Flow around rectangular cylinders: pressure forces and wake frequencies. *J. Wind Eng. Ind. Aerodyn.*, 49:187–196, 1993.

[34] H. Ouvrard, S. Wornom, B. Koobus, M.V. Salvetti, S. Camarri, and A. Dervieux. Computation of complex unsteady flows around bluff bodies through vms-les modeling. In *Proceedings of WEST-EAST HIGH SPEED FLOW FIELD CONFERENCE*, November 2007.

[35] W. Rodi, J. H. Ferziger, M. Breuer, and M. Pourquié. Status of large eddy simulation: results of a workshop. *ASME J. Fluids Eng.*, 119:248–262, 1997.

[36] P.L. Roe. Approximate Riemann solvers, parameters, vectors and difference schemes. *J. Comp. Phys.*, 43:357–372, 1981.

[37] J.W. Schewe. On the forces acting on a circular cylinder in cross flow from subcritical up to transcritical Reynolds numbers. *J. Fluid Mech.*, 133:265–285, 1983.

[38] S. Schmidt and F. Thiele. Comparison of numerical methods applied to the flow over wall-mounted cubes. *Int. J. of Heat and Fluid Flow*, 23:330–339, 2002.

[39] J. Smagorinsky. General circulation experiments with the primitive equations. *Monthly Weather Review*, 91(3):99–164, 1963.

[40] A. Sohankar, L. Davidson, and C. Norberg. Large eddy simulation of flow past a square cylinder: comparison of different subgrid scale models. *ASME J. Fluids Eng.*, 122:39–47, 2000.

[41] P.R. Spalart, W.H. Jou, M. Strelets, and S. Allmaras. *Advances in* DNS/LES, chapter Comments on the feasibility of LES for wings and on a hybrid RANS/LES approach. Columbus (OH), 1997.

[42] J.L. Steger and R.F. Warming. Flux vector splitting for the inviscid gas dynamic equations with applications to the finite difference methods. *J. Comp. Phys*, 40(2):263–293, 1981.

[43] A. Travin, M. Shur, M. Strelets, and P. Spalart. Detached-eddy simulations past a circular cylinder. *Flow, Turbulence and Combustion*, 63:293–313, 1999.

[44] B. van Leer. Towards the ultimate conservative scheme. IV: A new approach to numerical convection. *J. Comp. Phys.*, 23:276–299, 1977.

[45] A.W. Vreman. An eddy-viscosity subgrid-scale model for turbulent shear flow: algebraic theory and application. *Physics of Fluids*, 16:3670–3681, 2004.